



Research progress and the prospect of CO₂ hydrogenation with dielectric barrier discharge plasma technology

Ziyi Zhang¹ · Honglei Ding^{1,2,3,4} · Qi Zhou^{1,5} · Weiguo Pan^{1,2,3,4} · Kaina Qiu¹ · Xiaotian Mu¹ · Junchi Ma¹ · Kai Zhang¹ · Yuetong Zhao¹

Received: 18 October 2022 / Revised: 6 March 2023 / Accepted: 9 March 2023 / Published online: 18 May 2023
© The Author(s), under exclusive licence to Korean Carbon Society 2023

Abstract

In recent years, people are increasingly interested in CO₂ hydrogenation to produce value-added chemicals and fuels (CH₄, CH₃OH, etc.). In the quest for an efficient treatment in CO₂ methanation and methanolization, several technologies have been practiced, and DBD plasma technology gain attention due to its easily handling, mild operating conditions, strong activation ability, and high product selectivity. In addition, its reaction mechanism and the effect of packing materials and reaction parameters are still controversial. To address these problems efficiently, a summary of the reaction mechanism is presented. A discussion on plasma-catalyzed CO₂ hydrogenation including packing materials, reaction parameters, and optimizing methods is addressed. In this review, the overall status and recent findings in DBD plasma-catalyzed CO₂ hydrogenation are presented, and the possible directions of future development are discussed.

Keywords CO₂ · Hydrogenation · Dielectric barrier discharge · Plasma

1 Introduction

Since the Industrial Revolution, fossil resources have been fast depleted and lead to a continuous build-up of excessive CO₂ concentration in the atmosphere, which is the major contributor to global warming [1, 2]. It is showed in Fig. 1 that the trend of CO₂ content in the atmosphere since the 1960s. The CO₂ content is rising at an increasing rate which kept pace with the Global greenhouse effect. To restrain the impact, the intergovernmental panel on climate change (IPCC) recently recommend that the temperature

rise should be kept below 1.5 °C by 2100, which required a 45% reduction in greenhouse gas emissions by 2030 and zero emissions by 2050 [3]. Therefore, how to reduce the CO₂ effectively and environmentally friendly has become a research hotspot.

Up to now, considerable efforts have been devoted to develop innovative, stable and cost-effective technologies for treating CO₂. These technologies can be divided into two types: Carbon Capture and Storage (CCS) [4] and Carbon Capture and Utilization (CCU) [5, 6]. CCS is an effective method to reduce the concentration of CO₂ in the atmosphere in a short period, but it can't fundamentally solve the problem for the remaining CO₂ total amount [7, 8]. By comparison, CCU is a promising method based on CCS for CO₂ treatment, which brings CO₂ into the carbon cycle and converts it into value-added chemicals or fuels, thus reducing the total amount of CO₂. It is of great significance to the sustainable development of chemical and energy industries [9, 10]. Weatherbee et al. [11] studied the effect of reaction conditions and gas phase produced on CO₂ hydrogenation reaction as early as 1982, and put forward a conjecture on the kinetic reaction mechanism. Therefore, with the development of catalysts and processes, CCU will gradually become a mainstream technology for CO₂ treatment.

✉ Honglei Ding
hlding2005@163.com

¹ College of Energy and Mechanical Engineering, Shanghai University of Electric Power, Shanghai 200090, China

² Shanghai Power Environmental Protection Engineering Technology Research Center, Shanghai 201600, China

³ Key Laboratory of Environmental Protection Technology for Clean Power Generation in Machinery Industry, Shanghai 200090, China

⁴ Shanghai Non-carbon energy conversion and utilization institute, Shanghai 200240, China

⁵ Zhejiang Products Environmental Protection Energy Co, Hangzhou, China

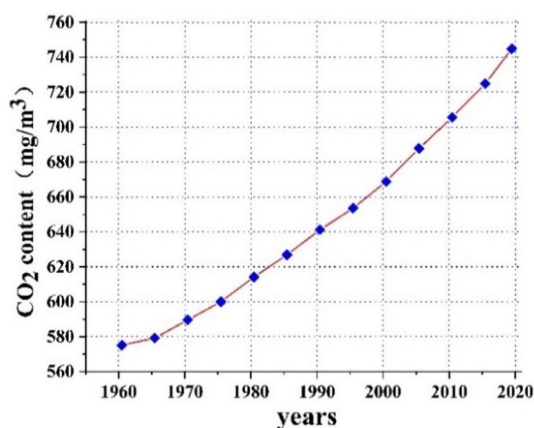


Fig. 1 Change trends of CO₂ content in the atmosphere in recent decades

CCU technologies mainly include thermocatalysis [12], photocatalysis [13, 14], biocatalysis [15–17], electrocatalysis [18–21] and plasma catalysis [22] etc. However, the high thermodynamic stability of CO₂ molecules ($\Delta G^\circ = -394 \text{ kJ}\cdot\text{mol}^{-1}$) is the greatest challenge for CCU [23]. Investigate its reason, it will spend plenty of energy to breakdown the C=O double bonds ($783 \text{ kJ}\cdot\text{mol}^{-1}$) [24] and dissociate the molecule during thermal activation process [25]. The energy efficiency is only 4.4% at a temperature of 300 K. The reaction does not start until the temperature rises to about 2000 K. The temperature needs to be raised to about 3000 K to reach 80% conversion and the energy efficiency is only 47%. [23]. The energy efficiency of photocatalysis is far from satisfactory. Electrocatalysis has higher energy efficiency and CO₂ conversion, and the modular reaction system is easy to scale amplification, but the product selectivity is lower. Biocatalysis has the high spatiotemporal yield and product selectivity, but it is limited by inactivation and high cost. Impressively, non-thermal plasma (NTP) technologies with non-thermodynamic equilibrium characteristics have shown some remarkable advantages in terms of CO₂ conversion [26], including low activation barrier, mild reaction conditions, fast reaction rate, and easy handling [27]. The ionized gas produced by plasma has a high activation ability, and is composed of electrons, free radicals, ions, photons, and excited states [28, 29]. These energetic species with an optimum range of electron energy is between 1 and 10 eV, which is used to activate CO₂ molecules by collision and dissociation under environmental conditions [30]. Besides, NTP is flexible in terms of the source of electricity, scalability both in size and applicability, and rarely relies on rare earth materials, etc. Thereby, plasma technology shows a great potential for CO₂ treatment [23].

According to the ways of the plasma produce, it can be classified as dielectric barrier discharge plasma (DBD), corona discharge, gliding arc discharge (GA), glow

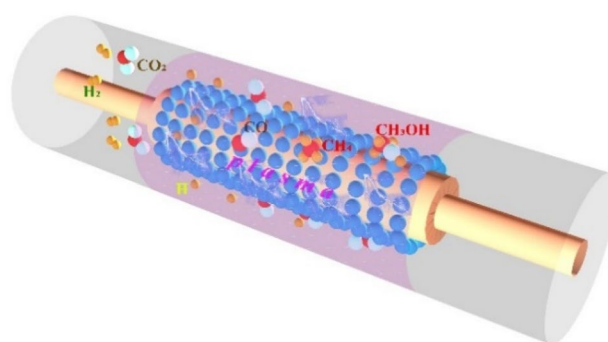


Fig. 2 Schematic diagram of DBD plasma reactor

discharge (GD), radio frequency (RF), and Microwave discharge (MW) [31, 32], etc. Among them, DBD plasma has become a research hotspot due to its wide range of pressure and discharge frequency, uniform discharge, and flexible combination with catalysts. By far, the methods of DBD CO₂ catalysis is mainly divided into CO₂ splitting [33, 34], carbon dioxide reforming of methane [35], and CO₂ hydrogenation [36]. Among them, the main products of CO₂ splitting are CO and O₂, and the by-products are the least [6]. Carbon dioxide reforming of methane requires a higher temperature. It is easy for coking and carbon deposition, and leads to the deactivation of catalyst and higher energy consumption [1]. Compared with formers, CO₂ hydrogenation is the most complicated and involves many reaction pathways. Due to the high reducibility of H₂, the high activation ability of plasma, and the synergistic effect between plasma and catalysts, it results in multiple reduction reactions of intermediate products and product diversification. The reaction mechanism and effect factors of CO₂ hydrogenation catalyzed by DBD plasma are still controversial, so a summary of the reaction mechanism is firstly presented in this review. Then, a discussion on plasma CO₂ hydrogenation including packing materials, react parameters, and optimize methods is addressed. Finally, this review presents the overall status and recent findings in DBD plasma-catalyzed CO₂ hydrogenation [36, 37].

2 Reaction mechanism of DBD plasma catalysis

The schematic diagram of the DBD plasma reactor is shown in Fig. 2. The inner electrode is a conductive steel rod, and the outer electrode is a conductive steel mesh. Non-conductive material (e.g. quartz glass) is inserted between them as the barrier medium. The outer electrode is powered by a high-voltage alternating current (AC) or pulse, supplying the energy to generate plasma. Interestingly, Ozkan et al. [38] has found that if the AC voltage was switched off at regular

times, a higher CO₂ conversion and energy efficiency will be obtained because of the lower gas temperature and the higher plasma voltage.

The electrons are heated selectively to be energetic electrons in the reacting area, with a suitable electron temperature of 10⁴ ~ 10⁵ K (1 ~ 10 eV) [39] to breakdown the reactants (CO₂ and H₂) by the ways of collision, dissociation, and ionization to produce ions, free radicals and excited molecules. These reactive species are catalyzed by the catalysts and quickly form new molecules such as CO, CH₄, and CH₃OH, etc. [28, 40]. Meanwhile, with the movement of these active species, the micro-discharge channels are formed and a non-spark stable discharge phenomenon is shown, which is named filamentary discharge. The insulating medium between the electrodes plays an important role in discharge storage, which restricts the discharge mode transition from filament discharge to spark discharge and improves the distribution of filament discharge in the whole electrode region [41, 42].

The possible reaction pathways of DBD plasma catalytic process for CO₂ hydrogenation without catalysts are shown in Table 1 [43] and Fig. 3. The thickness and the color of the arrow lines are proportional to the rate of the net reactions.

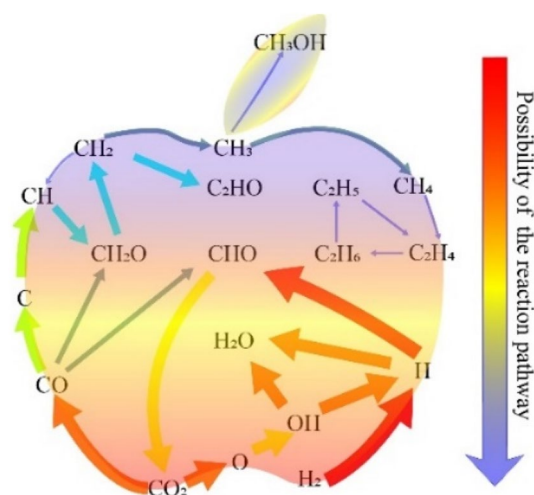


Fig. 3 Possible reaction pathway without catalysts in DBD plasma

The high-energy electron collisions lead to the dissociation of CO₂ and H₂, yielding CO, O, and H radicals. The recombination of O and H radicals forms OH radical, which further recombined into H₂O. The recombination of CO and H

Table 1 Main consumption and production pathway of main reactants involved in CO₂ hydrogenation in the DBD plasma process [44]

Molecule	Consumption reactions	Production reactions
CO ₂	$e^- + \text{CO}_2 \rightarrow 2e^- + \text{CO} + \text{O}$ $e^- + \text{CO}_2 \rightarrow e^- + \text{CO} + \text{O}$ $e^- + \text{CO}_2 \rightarrow \text{O}^- + \text{CO}$ $\text{CO}^+ + \text{CO}_2 \rightarrow \text{CO} + 2 + \text{CO}$	$\text{O} + \text{CHO} \rightarrow \text{H} + \text{CO}_2$ $\text{CO} + \text{OH} \rightarrow \text{CO}_2 + \text{H}$ $\text{CO} + 2 + \text{H}_2\text{O} \rightarrow \text{H}_2\text{O}^+ + \text{CO}_2$
H ₂	$e^- + \text{H}_2 \rightarrow e^- + \text{H} + \text{H}$ $e^- + \text{H}_2 \rightarrow 2e^- + \text{H} + 2$ $\text{H} + 2 + \text{H}_2 \rightarrow 2e^- + \text{H} + 3 + \text{H}$ $\text{H}_2\text{O} + \text{H}_2 \rightarrow \text{H}_3\text{O}^+ + \text{CO}_2$ $\text{H}_2 + \text{OH} \rightarrow \text{H} + \text{H}_2\text{O}$	$e^- + \text{H}_3\text{O}^+ \rightarrow \text{OH} + \text{H}_2$ $\text{H} + 3 + \text{H}_2\text{O} \rightarrow \text{H}_3\text{O}^+ + \text{H}_2$ $\text{H} + \text{H} + \text{M} \rightarrow \text{H}_2 + \text{M}$ $\text{H} + \text{CHO} \rightarrow \text{H}_2 + \text{CO}$
CO	$\text{H} + \text{CO} + \text{M} \rightarrow \text{CHO} + \text{M}$ $\text{CO} + \text{OH} \rightarrow \text{CO}_2 + \text{H}$ $e^- + \text{CO} \rightarrow e^- + \text{C} + \text{O}$	$\text{O} + \text{CHO} \rightarrow \text{CO} + \text{OH}$ $\text{CO}^+ + \text{CO}_2 \rightarrow \text{CO} + 2 + \text{CO}$ $e^- + \text{CO} + 2 \rightarrow \text{CO} + \text{O}$ $e^- + \text{CO}_2 \rightarrow \text{CO} + \text{O}^-$ $e^- + \text{CO}_2 \rightarrow e^- + \text{CO} + \text{O}$ $\text{H} + \text{CHO} \rightarrow \text{H}_2 + \text{CO}$
CH ₄	$\text{H} + 3 + \text{CH}_4 \rightarrow \text{CH} + 5 + \text{H}_2$ $\text{CO} + 2 + \text{CH}_4 \rightarrow \text{CH} + 4 + \text{CO}_2$ $e^- + \text{CH}_4 \rightarrow e^- + \text{CH}_3 + \text{H}$ $e^- + \text{CH}_4 \rightarrow 2e^- + \text{CH} + 4$ $\text{CH}_4 + \text{CH} \rightarrow \text{C}_2\text{H}_4 + \text{H}$ $e^- + \text{CH}_4 \rightarrow 2e^- + \text{H} + \text{CH} + 3$ $\text{CH} + 3 + \text{CH}_4 \rightarrow \text{C}_2\text{H} + 5 + \text{H}_2$ $e^- + \text{CH}_4 \rightarrow e^- + \text{CH}_2 + \text{H}_2$ $e^- + \text{CH}_4 \rightarrow e^- + \text{CH} + \text{H}_2 + \text{H}$ $\text{H}_2\text{O}^+ + \text{CH}_4 \rightarrow \text{H}_3\text{O}^+ + \text{CH}_3$	$\text{CH} + 5 + \text{H}_2\text{O} \rightarrow \text{H}_3\text{O}^+ + \text{CH}_4$ $\text{CH}_3 + \text{H} + \text{M} \rightarrow \text{CH}_4 + \text{M}$
CH ₃ OH	$\text{H} + \text{CH}_3\text{OH} \rightarrow \text{CH}_2\text{OH} + \text{H}_2$ $\text{H} + \text{CH}_3\text{OH} \rightarrow \text{CH}_3\text{O} + \text{H}_2$ $\text{OH} + \text{CH}_3\text{OH} \rightarrow \text{CH}_2\text{OH} + \text{H}_2\text{O}$ $\text{O} + \text{CH}_3\text{OH} \rightarrow \text{CH}_2\text{OH} + \text{OH}$ $\text{OH} + \text{CH}_3\text{OH} \rightarrow \text{CH}_3\text{O} + \text{H}_2\text{O}$ $\text{O} + \text{CH}_3\text{OH} \rightarrow \text{CH}_3\text{O} + \text{OH}$	$\text{H}_2\text{O} + \text{CH}_3\text{O} \rightarrow \text{CH}_3\text{OH} + \text{OH}$ $\text{H} + \text{CH}_2\text{OH} + \text{M} \rightarrow \text{CH}_3\text{OH} + \text{M}$ $\text{CH}_3 + \text{OH} + \text{M} \rightarrow \text{CH}_3\text{OH} + \text{M}$

is much more complex, the formed radicals will keep hydrogenating till to stable compounds such as CH_4 , and CH_3OH . Fortunately, these reactions can be simplified by catalysts. For instance, Ni-based catalysts show better catalyst activity in CO_2 methanation [44]. Cu-based catalysts show better catalyst activity in CO_2 methanolization [9].

3 Effects and optimizations

In the studies on DBD plasma-catalyzed CO_2 hydrogenation, researchers found that the optimizations of packing material properties, reaction parameters, and reactor structure should be a balance between higher CO_2 conversion and energy efficiency, and it will be discussed in detail in this section.

3.1 Packing materials

Many researches have been conducted on packing materials for DBD plasma assisting CO_2 hydrogenation. It has been found that the packed DBD plasma reactor shows a higher CO_2 conversion and energy efficiency than the nonpacked reactor [45–47]. It is ascribed to the permittivity [48], particle size, acid-base, and structure of packing materials. These parameters optimized the reactor system and changed the discharge mode from uniform space discharge to surface discharge to gain more energetic electrons and current under the same conditions.

The permittivity of the packing materials is one of the most important parameters influencing the DBD plasma catalytic process for CO_2 hydrogenation. The higher permittivity, the more energetic electrons and active free radicals will be generated in the packing materials under the same reaction condition [49], thus it can improve CO_2 conversion and energy efficiency. Mora et al. [50] has found that alumina shows better catalytic performances than quartz, which is due to the higher relative dielectric permittivity coefficient of alumina.

The particle size is another parameter of packing material. The particles near the contact point of the electrode formed a higher electric field and were easier to discharge [51]. The larger the particles, the higher the void fraction, which reduced the number of active species and energetic electrons and resulted in a decline in CO_2 conversion [52, 53]. Duan et al. [45] has found that appropriately increasing the alkalinity of the packing materials facilitates CO_2 adsorption, thus promoting CO_2 conversion. They also explored the structure of packing materials, and found that the packing materials of fiber structure contribute to a higher CO_2 conversion because the sharp edge morphology increased the intensity of micro-discharge filaments [54].

Packing the thermostable, conductive, and fibrous structure materials in a DBD reactor will further strengthen

the electrified and give birth to more energetic electrons. Hence, the higher chance of collisions obtained between high-energy electrons and reactive materials led to higher CO_2 conversion and energy efficiency.

3.2 Reaction parameters of DBD plasma system

The reaction parameters of DBD plasma-catalyzed CO_2 hydrogenation mainly include discharge power, discharge frequency, discharge length, feed flow rate, discharge gap, etc.

3.2.1 Discharge power

Energy is one of the most important factors influencing the hydrogenation of CO_2 by DBD plasma. As shown in Fig. 4, the enhancement of discharge power increased the numbers and the energy levels of active radicals and energetic electrons in the reaction area [55]. It improved the collision probability of reactants and plasma, thus forming more discharge channels and promoting CO_2 conversion [45]. However, there was a limitation on CO_2 conversion with increasing the discharge power, as the electrode surface has been covered by the micro-discharge filaments. The CO_2 conversion had little change, but energy efficiency was decreased. In addition, increasing the discharge power would cause higher heat loss in the whole reactor, which reduced energy efficiency [56, 57].

3.2.2 Discharge frequency

To explore the effect of reaction parameters on CO_2 conversion, researchers found that the discharge frequency affected CO_2 conversion and energy negligibly efficiency [24, 60]. It was ascribed to the fact that the modulation of discharge frequency mainly changed the motion path of plasma, but hardly influenced the number and average lifetime of micro discharges. However, discharge frequency played a main factor in vibration activation CO_2 , due to its effects on the

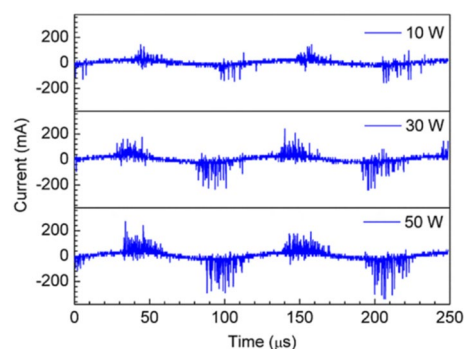


Fig. 4 Effect of discharge power on current signals [58]

voltage of gas gap [60] and the improvement of the resonance oscillation [25]. Some researchers also found that CO₂ conversion and energy efficiency decreased slightly with the increase in frequency, and it may be caused by the decrease in gas voltage [61].

3.2.3 Discharge length

With the increasing discharge length, the residence time of species in the discharge area will be prolonged, and the collision chance between reactive gas and energetic electrons or active free radicals will be increased. It would improve CO₂ conversion and energy efficiency (as shown in Fig. 5). However, the increasing discharge length can also reduce the discharge voltage and energy density. The effect of discharge length on CO₂ conversion rate and energy utilization efficiency presented as a parabola, so there was an optimal discharge length [13].

3.2.4 Feed flow rate

The influence of feed flow rate relates to the residence time of reactants in the reaction area (shown in Fig. 6). The collision chance of CO₂ molecules with energetic electrons and active radicals is decreased, but the absolute CO₂ conversion is increased because the availability of input energy is promoted. Higher energy efficiency and lower CO₂ conversion can be gotten with an increase in feed flow rate. As the feed flow rate increases, some of the energy was wasted in raising the reactor temperature and gas temperature, but the impact on energy efficiency was not significant [24].

3.2.5 Discharge gap

Due to the formation of high-energy micro discharged with increasing of the discharge gap [62], CO₂ conversion and

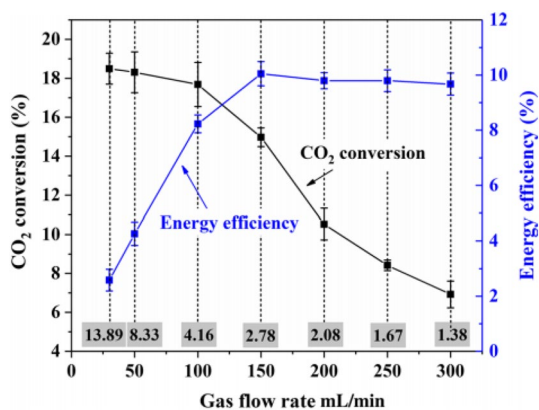


Fig. 5 the effect of gas flow rate on CO₂ conversion (the data at the bottom of the figure is SEI value)

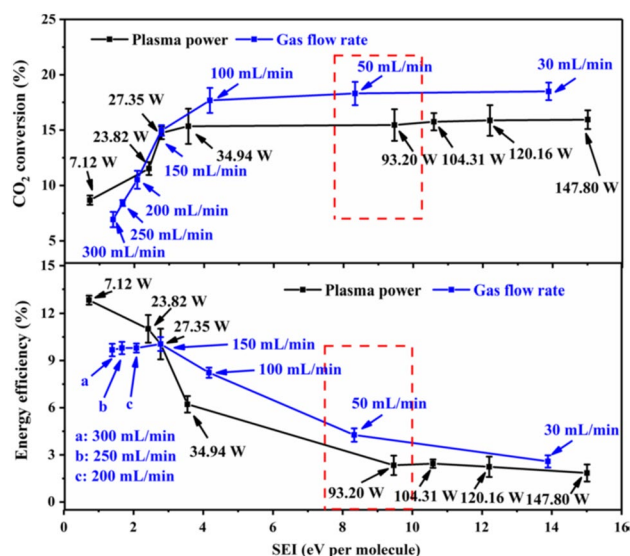


Fig. 6 Effects of SEI and residence time on CO₂ conversion and energy efficiency [33]

energy efficiency should be decreased, overall power consumption increased, and the number of active species and energetic electrons decreased. Besides, the collision probability and frequency among CO₂ molecules, active species, and energetic electrons was reduced, and this led to a further decline in CO₂ conversion efficiency [41].

Tu et al. [58] studied the influences of reaction parameters on the CO₂ conversion process. They found that the discharge power and feed flow rate were the main factors that affected CO₂ conversion. The influence degree of different reaction parameters on CO₂ conversion compared as q (feed flow rate) $\approx P$ (discharge power) $> dg$ (discharge gap) $> L$ (discharge length) $> f$ (discharge frequency), and that of the energy efficiency as $P > q > dg > L > f$. In addition, they noted that the minimum breakdown voltage and the peak operating voltage were the two most important parameters, and needed to be measured in the DBD process.

The DBD plasma-catalyzed CO₂ hydrogenation is affected by a number of interrelated factors. Although the relationships among these factors are complicated, there are two evaluation criteria, SEI (specific energy input) and residence time, respectively. SEI represented the average energy of particles in the reaction area and was defined as Equations R1 and R2, which were mainly determined by discharge power, discharge gap and discharge frequency. The residence time of molecules affected the collision probability and frequency of the reactants with energetic electrons in the reacting area, significantly influencing the CO₂ conversion. It was mainly determined by the discharge gap, discharge length, and feed flow rate [59]. Their relationships is shown in Fig. 7. Higher SEI, which improved the CO₂ conversion efficiency, could be

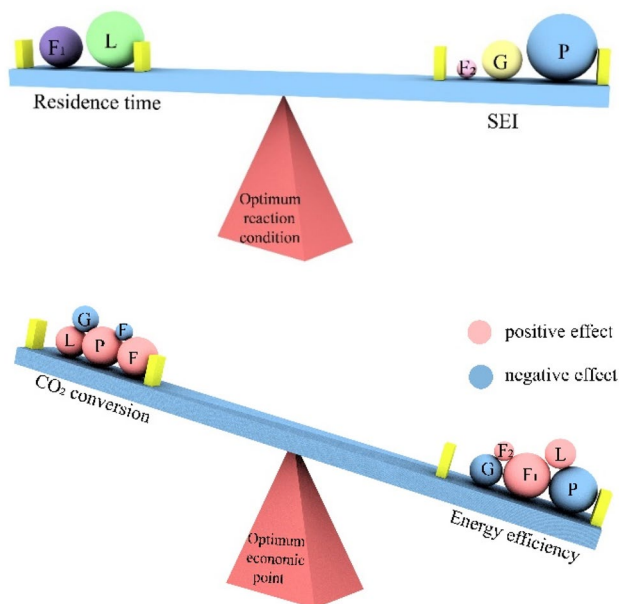


Fig. 7 **a** Optimum reaction condition; **b** Optimum economic point (F_1 Flow rate; L discharge length; F_2 discharge frequency; G discharge gap; P discharge power)

obtained by increasing the discharge power, narrowing the discharge gap, reducing the feed flow rate, and shortening the discharge length. However, the energy efficiency was decreased due to less residence time and heat loss. On the contrary, longer residence time will reduce SEI, which decreased energy efficiency as well as the CO_2 conversion was increased. Therefore, there was an optimum reaction condition point between SEI and residence time, it was one of the guiding theories to realize the industrialization of DBD plasma-catalyzed CO_2 hydrogenation. However, limited by the performance of the DBD reaction system, it was much more difficult to improve energy efficiency than CO_2 conversion. Therefore, there was an optimum economic point as shown in Fig. 7. It could be expected that future researches focused on optimizing the CO_2 conversion will be more than that on optimizing the energy efficiency.

The relationship between SEI formula and reaction parameters is as follows:

Specific energy input(SEI):

$$SEI\left(\frac{\text{kJ}}{\text{ml}}\right) = \frac{P(\text{KW})}{F(\text{ml/min})} \quad (\text{R1})$$

$$SEI\left(\frac{\text{eV}}{\text{mol}}\right) = SEI\left(\frac{\text{kJ}}{\text{ml}}\right) \frac{6.241 \times 10^{21} \times V_{\text{mol}}}{N_A} \quad (\text{R2})$$

P is power, F is feed flow rate; V_{mol} is the molar volume at a given pressure and temperature; N_A is Avogadro's constant.

3.3 Optimization of DBD system

It would be very complicated to improve both CO_2 conversion and energy efficiency only by adjusting reaction parameters, packed materials, and optimizing catalysts. There are many factors involved to restrict the relationship between SEI and residence time. It is a mutual-beneficial solution to improve SEI and residence time simultaneously, which is to optimize the reaction system. The specific solutions are as follows.

- (1) Multiple parallel electrode plasma reactor. Compared with the traditional DBD reactor, this type of reactor could produce more edge effects to form a wilder electric field, then give birth to more energetic electrons and active radicals, increase the number of the discharge channels, and promote CO_2 hydrogenation and energy efficiency [33].
- (2) Water electrode DBD reactor [9]. The gas temperature was raised when plasma catalyzes CO_2 hydrogenation, and the higher gas temperature should let to an expansion of gas and a decrease of the gas density. This will result in a reduction in residence time and energy efficiency against hydrocarbon generation. It is water, which circulate between internal and external cylinders in this type of reactor, act as a groundwater electrode, and absorb the heat emitted by the reactor as well as maintaining the react area temperature. This process could effectively reduce CO generation during the CO_2 hydrogenation process and improved energy efficiency.
- (3) The quartz glass reactor had better high-temperature resistance and chemical stability than the ordinary glass reactor.
- (4) Compared to ordinary steel mesh covers, the use of aluminum mesh as the outer electrode of the reactor helped the filter material reduce the leakage of ultraviolet light from the reactor, thus the light source was fully used [63].
- (5) Adding pure inert gas (e.g., N_2 , He , and Ar) into the DBD plasma reactor could promote CO_2 conversion [48], and the most commonly used inert gas is Ar . The addition of Ar made the discharge formed more easily and uniformly [64, 65], then increased the contact area and the synergistic effect between plasma and catalyst. Besides, the presence of Ar made a significant contribution to CO_2 conversion for the new reaction routes formed by the formation of metastable argon [66].
- (6) Regulating H_2/CO_2 ratio could significantly affect the product selectivity [62]. Appropriately increasing the H_2/CO_2 ratio will lead to an obvious improvement of CO_2 conversion, facilitate CH_4 and CH_3OH generation, but it's contrary to that of CO generation. A lower H_2/CO_2 was beneficial to generate CO , but the CO_2 conver-

sion, methanation and methanol were suppressed [67]. The energy efficiency decreased with the higher H₂/CO₂ ratio, because the hydrogen molecules competed with the CO₂ molecules in absorbing the energy supplied by plasma.

4 CO₂ hydrogenation to methane

The CO₂ methanation is shown in Fig. 8, also known as the Sabatier reaction, is considered as one of the most efficient CO₂ conversion methods. It provides a feasible way for the storage and utilization of renewable hydrogen and produces syngas. Besides, it is an essential part of the whole process of coal gasification to produce natural gas. Because CO₂ methanation is an 8-electron transfer

reaction, highly active metals, such as metals in groups VIII to X (Ru, Rh, Pd, Fe, Co, Ni, etc.), are usually selected to prepare catalysts. Nakayama et al. [68] prepared Ni/MgO catalysts with large Ni metal surface area. These Ni/MgO catalysts achieved NiO-MgO solid solution formation, and inhibited the aggregation of Ni metal particles as well as have high catalytic performance for CO₂ hydrogenation. In this review, plasma-catalyzed CO₂ hydrogenation Table 2 catalysts such as ruthenium-based catalysts, nickel-based catalysts, and hotspot catalyst MOF will be focused to be introduced.



4.1 Ruthenium-based catalyst

Ruthenium-based catalysts were considered as one of the most active CO₂ methanation catalysts due to their high catalytic activity and low reduction temperature. Lee et al. [41] used DBD plasma synergy Ru/γ-Al₂O₃ to catalyze CO₂ methanation, and confirmed that the presence of Ru affected the discharge characteristics of γ-Al₂O₃. The results of OES analysis showed that dielectric heating and electron collision were the major contributors to improve the efficiency of CO₂ methanation. Xu et al. [69] prepared Ru/MgAl-LDH to plasma-catalyzed methanation of CO₂ with CO₂ conversion of 85%. The CH₄ yield of the catalyst is 84%, the CO₂ conversion rate is 85%, which is about six times of the thermal catalytic CO₂ conversion at 250°C, and the activation barrier is one quarter of the thermal system. In addition, the synergistic effect between plasma and catalyst enhanced CO₂ hydrogenation at low temperatures.

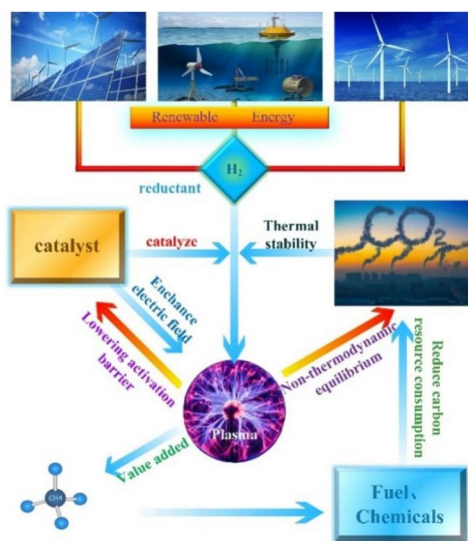


Fig. 8 CO₂ hydrogenation to methanation

Table 2 Reaction parameters and activity of several catalysts

Catalyst	F (kHz)	V (kV)	P (W)	T (°C)	Feed gas ^a	CH ₄ sell %	CH ₄ yield	CO ₂ conv %	References
Ru/γ-Al ₂ O ₃	3	9			7:1	97.38		23.2	[41]
Ru/MgAl-LDH	23.5	5			4:1		84%	85	[69]
15NiCZ5842						80	100%		[70]
Ni-Ce-Zr Hydrotalcite						80	≥ 99%		[71]
Ni/TiO ₂						73.2	Nearly 90%		[72]
15Ni-20La/Na-BETA	20.3	6		400		97		84	[73]
Ni/ZSM-5			14		3:1	87.9		46.3	[74]
Ru/Zr-MOF	7.1	19.2	13	4:1		94.6	39.1%	41.3	[75]
Ru@UiO-66			13	4:1	30	95.4		72.2	[76]
Ni/γ-Al ₂ O ₃				250		70		40	[77]

^aFeed gas: H₂/CO₂ molar ratio

^bEnergy efficiency

4.2 Nickel-based catalyst

Although noble metals exhibit excellent catalytic performance, their high prices have prompted researchers to open or find a new path or snap course. Nickel-based catalysts are one of the best replacements for noble metals, which have been extensively studied in DBD plasma-catalyzed CO₂ methanation due to the lower price, easily accessible, and excellent catalytic activity. Recent studies have shown that the catalytic performance of Ni-based catalysts for CO₂ methanation mainly depends on the support, nickel loading quantity, secondary metals, and preparation methods [78].

Different supports had a significant impact on the morphology of the active phase, adsorption, and catalytic properties of Ni-based catalysts [78]. To prepare highly dispersed supported metal catalysts, oxides with high surface area are usually used, such as Al₂O₃, SiO₂, TiO₂, CeO₂, La₂O₃, and zeolites. There were many factors that influence the performance of supported metal catalysts, including pore size, structure, surface chemistry, and strong metal support interaction (SMSI) [79]. Ni/ γ -Al₂O₃ was commonly used in the methanation of carbon dioxide with hydrogen. It has shown highly catalytic activity, but suffers severe carbon deposition and poor stability in high reaction temperature [80]. Jin et al. [81] pre-treated the precursor of Ni/ γ -Al₂O₃ by DBD plasma and founded the discharge power significantly impact the reducibility and catalytic activity of Ni/ γ -Al₂O₃. At the low discharge power, the precursor (nickel nitrate) did not obviously reduce and decompose into Ni oxides, but the catalytic activity, stability, and reducibility could be improved and stabilized at limit value with the increasing of power. It could be mainly ascribed to the smaller Ni particle size, more basic sites, weaker alkalinity and less prone to carbon deposition and sintering caused by plasma treatment. Sivachandiran et al. [77] used plasma to treat Ni/ γ -Al₂O₃ to catalyze CO₂ methanation in DBD. In this process, the catalytic temperature was 50°C to 250°C lower than that in conventional thermal catalysis, and it is observed that NiO is evenly dispersed on the surface of alumina beads. Plasma treatment could slightly increase the pore size of Ni, and 40% CO₂ conversion, and 70% CH₄ selectivity were reached, respectively. Jia et al. [82] prepared Ni/ZrO₂ by plasma decomposition of nickel precursor, which showed high dispersion and Ni(111) as the main lattice plane. Besides, an enhancement of the cooperation between Ni and interfacial active sites was achieved, and led to a faster dissociative adsorption of H₂ and hydrogen spillover. Therefore, sufficient H atoms were generated for CO₂ hydrogenation, which enhanced the generation of oxygen vacancies on ZrO₂ surface, then the oxygen vacancy further enhanced the adsorption and activation of CO₂, so that the excellent low temperature activity for CO₂ methanation could be obtained.

To further reflect the difference between thermal catalysis and plasma catalysis.

To overcome the sinterability of nickel-based catalysts in carbon dioxide methanation, the second metals like Fe, Zr, Co, La, Mg, etc. could be loaded to change the catalytic electronic distribution and geometric structure, which could improve the stability and catalytic activity of the nickel-based catalysts [83]. Li et al. [84] found that Fe can improve the catalytic performance of Ni/Al₂O₃ for CO₂ methanation, but the positive effect of adding Fe was volcanic and had an optimal point. Wierzbicki et al. [85] compared a series of bimetallic layered double hydroxide-derived materials containing a fixed amount of Ni and different amounts of Fe by coprecipitation. It was found that the introduction of Fe in the layered double hydroxyl group changed the interaction between Ni and the support matrix. After introducing a small amount of Fe, the number of medium bases increased sharply, but the weakly basic bases increased slightly. The number of high bases decreased when more Fe was introduced.

The catalyst performance of CO₂ methanation could be improved by improving the preparation method of the catalyst and the dispersion degree of the active site of the catalyst, which should be paid attention by researchers. Besides, although NTP-DBD cooperated with high temperature and showed excellent catalysis results, the high temperature favored CH₄ reforming to CO and H₂, and facilitated water gas reaction to produce CO [77].

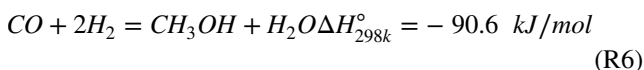
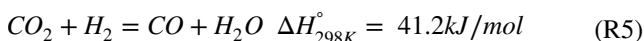
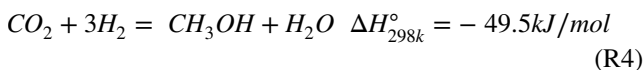
4.3 Metal–organic framework materials

Metal–organic framework (MOF) is a series of porous crystalline materials self-assembled by metal ions and organic ligands through coordination bonds. It has attracted much attention due to its high specific surface area, porosity, adjustable functional structure and CO₂ adsorption performance [86]. UiO-66 is a typical Zr-based MOF with a perfect frame structure and excellent thermal stability. The common carriers of UiO-66 are Cu, Au, Pd, Pt, Ru, etc. Xu et al. [75] prepared Zr-MOF loaded Ru with a solvothermal method to catalyze CO₂ methanation, and found that Ru³⁺ was oxidized to RuO in the reaction process. Thus, catalytic capacity showed better, and the selectivity and yield of CH₄ reached 94.6% and 39.1%, respectively. Xu et al. [76] used solvothermal method preparing UiO-66 loaded Ru nanoparticles (NPs) to catalyze CO₂ methanation under NTP-DBD, and no change was found after the loading of Ru in terms of the integrity of structure, crystallinity, specific surface area and thermal stability of UiO-66. Besides, the Ru NPs in Ru@UiO-66 had good dispersibility, unique frame structure, and the synergy with NTP-DBD, thus showing a better catalytic activity than UiO-66 and Ru/Al₂O₃, with CO₂ conversion of 72.2% and CH₄ selectivity 95.4%, respectively. Lan

et al. [74] studied the effect of ZSM-5 loaded different metals on CO₂ hydrogenation, and found that Cu/ZSM-5 cannot promote the generation of any hydrocarbons. Ni/ZSM-5, Fe/ZSM-5, and Mo/ZSM-5 promoted methane generation, and Ni/ZSM-5 showed the highest selectivity 90.5%. Co/ZSM-5 promoted C2-C4 formation with the highest C2-C4 selectivity of 13.7%.

5 CO₂ hydrogenation to methanol

To reduce CO₂ content in the atmosphere and the reliance of fossil resource, “methanol economy” [87, 88] gradually attracted special attention, as shown in Fig. 9. Methanol was not only an important raw material for chemical industries and a cleaner resource than fossil fuels [89], but also a good chemical storage carrier for H₂. It provided a solution for CO₂ utilization [90]. The reaction equations [91, 92] is shown below:



5.1 Photocatalysis

As one of the most important catalysts to catalyze CO₂ hydrogenation to methanol, copper-based catalysts have been greatly developed recently due to their higher activity and higher product selectivity [93]. For example, in the field of photocatalysis CO₂ methanol, Cu/ZnO is one of the most effective photocatalysts. Because ZnO improved the dispersion of Cu particles, the SMSI between Cu and

ZnO significantly improved the methanol selectivity. Cu was much higher than other crystal facets, so it had higher methanol selectivity [94, 95]. Further studies have found that adding appropriate amounts of CdSe, g-C₃N₄, Al³⁺, and Ca³⁺ into the Cu/ZnO will enhance the catalytic activity and the product selectivity. Among them, g-C₃N₄ was cheapest, non-toxic, and easiest to hybridize with ZnO. Deng et al. [96] prepared Cu/g-C₃N₄-ZnO/Al₂O₃ by modifying ZnO with g-C₃N₄, which showed a higher catalytic performance than traditional Cu/ZnO/Al₂O₃. Li et al. [97] found that adding a small amount of Ca³⁺ into the precursor of the Cu/ZnO catalyst will form gallium spinel ZnGa₂O₄, producing CuZn bimetallic nanoparticles, which could significantly improve the CO₂ conversion and methanol selectivity [98].

5.2 Electrocatalysis

In the field of electrocatalytic CO₂ methanol, copper was the only monometallic catalyst that could produce appreciable amounts of hydrocarbons [99]. The catalytic performance of Cu-based catalysts can be improved by the surface morphology of Cu electrodes, the electronic structure, the geometric and bonding properties between copper and metal substances. Different crystal faces of Cu exhibit different catalytic properties for CO₂ conversion. For example, Cu (111) favored the formation of COH*, which combined with CH₂ to produce methane and ethylene under high overpotential (< − 0.8 V-RHE). Under low overpotential (− 0.4 ~ 0.6 V-RHE), the Cu(100) favored the formation of CHO* and two CHO* species will couple to form ethylene [100]. However, at a high overpotential and CO* relative surface coverage, Cu(100) gave preference to generate COH* and produced CH₄ and CH₃OH via a similar reaction pathway as Cu(111) [101]. Jiao et al. [102] revealed that the g-C₃N₄ could be used as the molecular scaffold to appropriately modify the electronic structure of Cu in the resultant Cu-C₃N₄ and efficiently elevate the d-band position of Cu toward the Fermi level, thus significantly improved catalyst ability to activate CO₂ and adsorbing intermediate reactants. Moreover, for the first time, synergistic molecular catalysis with double active centers was found on the surface of Cu-C₃N₄. Ma et al. [103] has compared the performance of different types of bimetallic Cu-Pd catalysts such as ordered, disordered and phase-separated. They found that the order Cu-Pd showed the highest C1 selectivity, which suggested that the C1 intermediate was easier to dimerize on surface of neighboring Cu atoms and the geometric effect was key to determine Cu-Pd selectivity. Kattel et al. [104] compared the activity and selectivity of TiO₂/Cu and ZrO/Cu. They found that the source of the excellent promotion effect of ZrO₂ was related to the fine-tuning ability of Zr³⁺ reduction at the interface, which could appropriately combine the key reaction intermediates, such as *CO₂, *CO, *HCO and *

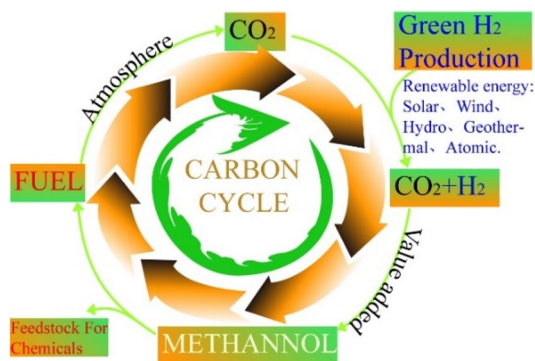


Fig. 9 Schematic diagram of methanol economy

H₂CO, to promote the formation of methanol. However, the current research progress of Cu-based catalyst forelectrocatalytic CO₂ methanol is still in the basic research stage, focusing on solving the problems to get higher overpotential required for the reaction, lower Faraday efficiency, lower product selectivity and faster deactivation.

5.3 Plasma catalysis

Despite many technologies mentioned above have been well-developed for CO₂ hydrogenation to methanol, they still face many challenges. One of the major challenges is the high reaction pressure. According to the reaction thermodynamics, CO₂ hydrogenation to methanol (Eq. R4) is an exothermic and molecule-reducing reaction, which is favored to occur at lower temperatures and higher pressure [105]. However, lower temperature operation is a subject to a thermodynamic equilibrium limitation in CO₂ activation. Although higher temperature facilitates CO₂ activation, the simultaneous formation of CO (Eq. R4) is promoted, which is the primary competitive reaction with Eq. R3. DBD plasma technology with non-thermodynamic equilibrium provides an attractive method to produce methanol at atmospheric temperature and pressure. For example, Wang et al. [9] used a water-electrode DBD reactor to compare the catalytic performance of Cu/γ-Al₂O₃ and Pt/γ-Al₂O₃ in terms of CO₂ conversion and methanol yield, and found that the Cu/γ-Al₂O₃ had a stronger catalytic activity and achieved a CO₂ conversion of 21.2%, a methanol yield of 11.3%. They also found that the methanol produced was strongly dependent on the DBD plasma reactor configuration. Luo et al. [14] found that Cu/ZnO/C prepared by cold plasma treatment had higher dispersion, smaller particle size and lower agglomeration, and higher CO₂ adsorption capacity than the catalyst prepared by calcination. The plasma treatment also introduced specific oxygen-containing groups to the activated carbon, which facilitated hydrogen spillover onto the catalyst. Besides, plasma promoted the formation of ZnO (002) planes, which exhibited higher surface energy and a stronger SMSI with Cu than that of other crystal facet, thus promoting the activation and hydrogenation of CO₂.

DBD plasma catalyzes CO₂ hydrogenation to methanol is rarely reported recently. Analysis of the following reasons: (1) The water formed during CO₂ hydrogenation leads to catalysts deactivation, and would absorb a large amount of energy and blocked the movement of high energetic electrons. It results in the CO₂ conversion and energy efficiency reduced. (2) The reaction pathways of CO₂ hydrogenation to methanol are very complex (as shown in Fig. 4 and Table 1), and lots of by-products should easily generate. (3) At room temperature, the methanol is liquid, which is easy to adhere to the reactor, gas pipeline and GC, etc. It may result in errors in data calculation, and easily cause pollution and

damage to the reaction system [9]. (4) Compared with the atmospheric operation conditions of DBD plasma-catalyzed CO₂ hydrogenation, this reaction (Equation R3) is a phase change (from gas to liquid) process, so the impact of higher pressure is greater than atmospheric conditions. To address the problems, the research and development of a new reactor system would become the top priority.

6 Conclusion

In this review, the reaction mechanism of DBD plasma-catalyzed CO₂ hydrogenation is described in detail. It is a process of gradual hydrogenation, and the final products are mainly influenced by the H₂/CO₂ ratio and the catalyst types. For example, a lower H₂/CO₂ ratio is easier to produce CO, while a higher H₂/CO₂ ratio is easier to produce CH₄ and CH₃OH, etc. Ni-based catalysts promote the formation of methane. Copper-based catalyst promotes the formation of methanol. CO₂ conversion and energy efficiency are important indicators for DBD economic evaluation. Their influencing factors and optimization measures as follow.

- (1) Packing materials can improve discharge mode from filamentous discharge to the combination of surface discharge and filamentous discharge, which increases the amount of high energetic electrons, active species, and free radicals, and thus improves the CO₂ conversion and energy efficiency. Specifically, a good performance is found in the materials with high specific surface area, fiber and high dielectric constant.
- (2) The SEI and residence time can be used as the evaluation criteria to adjust the reaction parameters such as discharge voltage, discharge length, discharge gap, discharge frequency and feed flow rate, so as to obtain the optimum reaction parameters.
- (3) Optimization of the reaction system can improve both SEI and residence time, so as to improve CO₂ conversion and energy efficiency at the same time. This is a very good method, but it still needs theoretical breakthrough and innovation. At present, relatively good reaction systems included multiple external electrodes in parallel, hydroelectric poles, rhombus aluminum grid reactors, etc. In addition, adding inert gas, such as Ar, is a useful measure too.

Based on the presented researches above, the further study directions of DBD catalyzed CO₂ hydrogenation to methane or methanol are proposed as follow.

- (1) CO₂ methanation. Recently, the research mainly involved Ruthenium-based catalysts, Nickel-based catalysts, and MOF. Ruthenium catalysts showed the

best reactivity, but its price is the highest. MOF had a higher specific surface area, porosity, CO₂ adsorption, and adjustable functional structure, but its preparation is difficult. Most research reported on Ni-based materials and mainly focused on the supports, nickel loading, secondary metals and preparation methods. The goal is to improve the pore diameter, structure, surface chemical properties and the SMSI, and subsequently to enhance catalyst stability, CO₂ adsorption, catalytic activity and dispersion degree of active components as well as reduce the carbon deposition and sintering phenomenon. In addition, the catalyst prepared by the plasma system generally showed a better performance of CO₂ conversion and methane selectivity, which was a promising method.

- (2) CO₂ methanolization. Copper-based catalysts, as the main catalysts for CO₂ methanolization, have been developed well in recent years. In the field of photocatalysis, Cu/ZnO is one of the most important catalysts, and the SMSI between Cu and ZnO is further studied. It was also found that CdSe, g-C₃N₄, Al³⁺, and Ca³⁺ could further improve the yield and selectivity of the products. Recent studies in the field of electrocatalysis showed that the catalytic performance of copper-based catalysts could be improved by studying the surface morphology, electronic structure, geometric structure, and bonding performance of copper and metal materials of copper electrodes. It is the guiding theory to solve the problems of high overpotential, low Faraday efficiency, low product selectivity, and rapid deactivation. Compared with the formers, DBD plasma technology with non-thermodynamic equilibrium characteristics has a great potential on CO₂ methanol in theory. The reason might be the long reaction pathway during which water is generated and then leads to catalyst deactivation. At the same time, the generated methanol is easy to condense and adhere to the reactor and gas pipe. Besides, the reaction condition is low pressure and the stimulating effect on the phase transition reaction is weaker than high pressure. The performance of DBD plasma-catalyzed CO₂ methanolization places a strong requirement on the design and structure of the reaction system. Therefore, in addition to the development of high-performance catalysts, optimization of the reaction system will be an essential step, which should be taken seriously by researchers.

Acknowledgements We acknowledge support from Subproject of National Key Research and Development Program (2018YFB0604204) and Shanghai Science and Technology Project (21DZ1207200).

Shanghai University of Electric Power, Yangpu District, 200090, Ziyi zhang.

Data availability Data sharing is not applicable to this article as no new data were created or analyzed in this study.

Declarations

Conflict of interest The authors declare that they have no known competing financial interests or personal relationships that could have appeared to influence the work reported in this article.

References

- Mikkelsen M, Jorgensen M, Krebs FC (2010) The teraton challenge. A review of fixation and transformation of carbon dioxide. *Energy Environ Sci* 3:43–81. <https://doi.org/10.1039/B912904A>
- Li S, Guo L, Ishihara T (2019) Hydrogenation of CO₂ to methanol over Cu/AlCeO catalyst. *Catal Today*. <https://doi.org/10.1016/j.cattod.2019.01.015>
- Chen W, Yan S (2022) The decoupling relationship between CO₂ emissions and economic growth in the Chinese mining industry under the context of carbon neutrality. *J Cleaner Prod* 379:134692. <https://doi.org/10.1016/j.jclepro.2022.134692>
- Sgouridis S, Carbajales-Dale M, Csala D, Chiesa M, Bardi U (2019) Comparative net energy analysis of renewable electricity and carbon capture and storage. *Nat Energy* 4:456–465. <https://doi.org/10.1038/s41560-019-0365-7>
- Mac Dowell N, Fennell PS, Shah N (2017) Maitland, The role of CO₂ capture and utilization in mitigating climate change. *Nat Clim Change* 7:243–249. <https://doi.org/10.1038/NCLIMATE3231>
- Bhatia SK, Bhatia RK, Jeon JM, Kumar G, Yang YH (2019) Carbon dioxide capture and bioenergy production using biological system - A review. *Renew Sustain Energy Rev* 110:143–158. <https://doi.org/10.1016/j.rser.2019.04.070>
- Singh G, Lee J, Karakoti A, Bahadur R, Yi J, Zhao D, AlBahily K (2020) Vinu, Emerging trends in porous materials for CO₂ capture and conversion. *Chem Soc Rev*. <https://doi.org/10.1039/D0CS00075B>
- Bui M, Adjiman CS, Bardow A, Anthony EJ, Boston A, Brown S, Fennell PS, Fuss S, Galindo A, Hackett LA, Hallett JP, Herzog HJ, Jackson G, Kemper J, Krevor S, Maitland GC, Matuszewski M, Metcalfe IS, Petit C, Puxty G, Reimer J, Reiner DM, Rubin ES, Scott SA, Shah N, Smit B, Trusler JPM, Webley P, Wilcox J, Mac Dowell N (2018) Carbon capture and storage (CCS) the way forward. *Energy Environ Sci* 11:1062–1176. <https://doi.org/10.1039/C7EE02342A>
- Wang L, Yi Y, Guo H, Tu X (2017) Atmospheric pressure and room temperature synthesis of methanol through plasma-catalytic hydrogenation of CO₂. *ACS Catal* 8:90–100. <https://doi.org/10.1021/acscatal.7b02733>
- Di Chiara A, Chiarella F, Savonitto S, Lucci D, Bolognese L, De Servi S, Greco C, Boccanelli A, Zonzin P, Coccolini S, Maggioni AP, Investigators B (2003) Epidemiology of acute myocardial infarction in the Italian CCU network: the BLITZ study. *Eur Heart J* 24:1616–1629. [https://doi.org/10.1016/S0195-668X\(03\)00278-1](https://doi.org/10.1016/S0195-668X(03)00278-1)
- Weatherbee GD, Bartholomew CH (1982) Hydrogenation of CO₂ on group VIII metals: II. Kinetics and mechanism of CO₂ hydrogenation on nickel. *J Catal* 77:460–472. [https://doi.org/10.1016/0021-9517\(82\)90186-5](https://doi.org/10.1016/0021-9517(82)90186-5)
- Lee WJ, Li C, Prajitno H, Yoo J, Patel J, Yang Y, Lim S (2020) Recent trend in thermal catalytic low temperature CO₂ methanation: A critical review. *Catal Today*. <https://doi.org/10.1016/j.cattod.2020.02.017>

13. Ting KW, Toyao T, Siddiki SMAH, Shimizu K (2019) Low-temperature hydrogenation of CO₂ to methanol over heterogeneous TiO₂-supported re catalysts. *ACS Catal* 9:3685–3693. <https://doi.org/10.1021/acscatal.8b04821>
14. Li YY, Wei ZH, Fan JB, Li ZJ, Yao HC (2019) Photocatalytic CO₂ reduction activity of Z-scheme CdS/CdWO₄ catalysts constructed by surface charge directed selective deposition of CdS. *Appl Surf Sci* 483:442–452. <https://doi.org/10.1016/j.apsusc.2019.03.333>
15. Alissandratos A, Easton CJ (2015) Biocatalysis for the application of CO₂ as a chemical feedstock. *Beilstein J Org Chem* 11:2370–2387. <https://doi.org/10.3762/bjoc.11.259>
16. Wang Y, Li M, Zhao Z, Liu W (2015) Effect of carbonic anhydrase on enzymatic conversion of CO₂ to formic acid and optimization of reaction conditions. *J Mol Catal B Enzym* 116:89–94. <https://doi.org/10.1016/j.molcatb.2015.03.014>
17. Appel AM, Bercaw JE, Bocarsly AB, Dobbek H, DuBois DL, Dupuis M, Ferry JG, Fujita E, Hille R, Kenis PJ, Kerfeld CA, Morris RH, Peden CH, Portis AR, Ragsdale SW, Rauchfuss TB, Reek JN, Seefeldt LC, Thauer RK, Waldrop GL (2013) Frontiers, opportunities, and challenges in biochemical and chemical catalysis of CO₂ fixation. *Chem Rev* 113:6621–6658. <https://doi.org/10.1021/cr300463y>
18. Kattel S, Yu W, Yang X, Yan B, Huang Y, Wan W, Liu P, Chen JG (2016) CO₂ Hydrogenation over oxide-supported PtCo catalysts: the role of the oxide support in determining the product selectivity. *Angew Chem* 55:7968–7973. <https://doi.org/10.1002/anie.201601661>
19. Li Q, Rao X, Sheng J, Xu J, Yi J, Liu Y, Zhang J (2018) Energy storage through CO₂ electroreduction A brief review of advanced Sn-based electrocatalysts and electrodes. *J CO₂ Util* 27:48–59. <https://doi.org/10.1016/j.jcou.2018.07.004>
20. Waldie KM, Flajlslik KR, McLoughlin E, Chidsey CE, Waymouth RM (2017) Electrocatalytic alcohol oxidation with ruthenium transfer hydrogenation catalysts. *J Am Chem Soc* 139:738–748. <https://doi.org/10.1021/jacs.6b09705>
21. Feng JP, Zeng SJ, Feng JQ, Dong HF, Zhang XP (2018) CO₂ electroreduction in ionic liquids: a review. *Chin J Chem* 36:961–970. <https://doi.org/10.1002/cjoc.201800252>
22. Ma X, Li S, Ronda-Lloret M, Chaudhary R, Lin L, van Rooij G, Gallucci F, Rothenberg G, Raveendran Shiju N, Hessel V (2018) Plasma assisted catalytic conversion of CO₂ and H₂O Over Ni/Al₂O₃ in a DBD Reactor. *Plasma Chem Plasma Process* 39:109–124. <https://doi.org/10.1007/s11090-018-9931-1>
23. Snoeckx R, Bogaerts A (2017) Plasma technology - a novel solution for CO₂ conversion? *Chem Soc Rev* 46:5805–5863. <https://doi.org/10.1039/C6CS00066E>
24. Aerts R, Somers W, Bogaerts A (2015) Carbon dioxide splitting in a dielectric barrier discharge plasma: a combined experimental and computational study. *Chemsuschem* 8:702–716. <https://doi.org/10.1002/cssc.201402818>
25. Lu N, Zhang C, Shang K, Jiang N, Li J, Wu Y (2019) Dielectric barrier discharge plasma assisted CO₂ conversion: understanding the effects of reactor design and operating parameters. *J Phys D Appl Phys* 52:224003. <https://doi.org/10.1088/1361-6463/ab0ebb>
26. Paulussen S, Verheyde B, Tu X, De Bie C, Martens T, Petrovic D, Bogaerts A, Sels B (2010) Conversion of carbon dioxide to value-added chemicals in atmospheric pressure dielectric barrier discharges. *Plasma Sources Sci Technol* 19:034015. <https://doi.org/10.1088/0963-0252/19/3/034015>
27. Tu X, Whitehead JC (2012) Whitehead, Plasma-catalytic dry reforming of methane in an atmospheric dielectric barrier discharge: Understanding the synergistic effect at low temperature. *Appl Catal B* 125:439–448. <https://doi.org/10.1016/j.apcatb.2012.06.006>
28. Dębek R, Azzolina-Jury F, Travert A, Maugé F (2019) A review on plasma-catalytic methanation of carbon dioxide – Looking for an efficient catalyst. *Renew Sust Energy Rev* 116:109427. <https://doi.org/10.1016/j.rser.2019.109427>
29. Bai YH, Chen JR, Li XY, Hang CH (2009) Non-thermal plasmas chemistry as a tool for environmental pollutants abatement. *Rev Environ Contam Toxicol* 201:117–136. https://doi.org/10.1007/978-1-4419-0032-6_4
30. Zhao T, Ullah N, Hui Y, Li Z (2019) Review of plasma-assisted reactions and potential applications for modification of metal—organic frameworks. *Front Chem Sci Eng* 13:444–457. <https://doi.org/10.1007/s11705-019-1811-6>
31. de la Fuente JF, Moreno SH, Stankiewicz AI, Stefanidis GD (2017) On the improvement of chemical conversion in a surface-wave microwave plasma reactor for CO₂ reduction with hydrogen (The Reverse Water-Gas Shift reaction). *Int J Hydrogen Energy* 42:12943–12955. <https://doi.org/10.1016/j.ijhydene.2017.04.040>
32. Chen G, Britun N, Godfroid T, Georgieva V, Snyders R, Delpiancke-Ogletree MP (2017) An overview of CO₂ conversion in a microwave discharge: the role of plasma-catalysis. *J Phys D Appl Phys*. <https://doi.org/10.1088/1361-6463/aa5616>
33. Niu GH, Qin Y, Li WW, Duan YX (2019) Investigation of CO₂ splitting process under atmospheric pressure using multi-electrode cylindrical DBD plasma reactor. *Plasma Chem Plasma Process* 39:809–824. <https://doi.org/10.1007/s11090-019-09955-y>
34. Belov I, Paulussen S, Bogaerts A (2016) Appearance of a conductive carbonaceous coating in a CO₂ dielectric barrier discharge and its influence on the electrical properties and the conversion efficiency. *Plasma Sour Sci Technol* 25:015023. <https://doi.org/10.1088/0963-0252/25/1/015023>
35. Singha RK, Yadav A, Agrawal A, Shukla A, Adak S, Sasaki T, Bal R (2016) Synthesis of highly coke resistant Ni nanoparticles supported MgO/ZnO catalyst for reforming of methane with carbon dioxide. *Appl Catal B* 191:165–178. <https://doi.org/10.1016/j.apcatb.2016.03.029>
36. Zhang K, Zhang G, Liu X, Phan AN, Luo K (2017) A study on CO₂ decomposition to CO and O₂ by the combination of catalysis and dielectric-barrier discharges at low temperatures and ambient pressure. *Ind Eng Chem Res* 56:3204–3216. <https://doi.org/10.1021/acs.iecr.6b04570>
37. Liu M, Yi Y, Wang L, Guo H, Bogaerts A (2019) Hydrogenation of carbon dioxide to value-added chemicals by heterogeneous catalysis and plasma catalysis. *Catalysts* 9:275. <https://doi.org/10.3390/catal9030275>
38. Ozkan A, Dufour T, Silva T, Britun N, Snyders R, Reniers F, Bogaerts A (2016) DBD in burst mode: solution for more efficient CO₂ conversion? *Plasma Sources Sci Technol* 25:055005. <https://doi.org/10.1088/0963-0252/25/5/055005>
39. Chen H, Mu Y, Shao Y, Chansai S, Xiang H, Jiao Y, Hardacre C, Fan X (2019) Nonthermal plasma (NTP) activated metal–organic frameworks (MOFs) catalyst for catalytic CO₂ hydrogenation. *AIChE J*. <https://doi.org/10.1002/aic.16853>
40. Bogaerts A, Berthelot A, Heijckers S, Kolev S, Snoeckx R, Sun S, Trenchev G, Van Laer K, Wang W (2017) CO₂ conversion by plasma technology: insights from modeling the plasma chemistry and plasma reactor design. *Plasma Sources Sci Technol* 26:063001. <https://doi.org/10.1088/1361-6595/aa6ada>
41. Lee CJ, Lee DH, Kim T (2017) Enhancement of methanation of carbon dioxide using dielectric barrier discharge on a ruthenium catalyst at atmospheric conditions. *Catal Today* 293:97–104. <https://doi.org/10.1016/j.cattod.2017.01.022>
42. Ozkan A, Dufour T, Bogaerts A, Reniers F (2016) How do the barrier thickness and dielectric material influence the filamentary mode and CO₂ conversion in a flowing DBD? *Plasma Sour Sci Technol* 25:045016. <https://doi.org/10.1088/0963-0252/25/4/045016>

43. De Bie C, van Dijk J, Bogaerts A (2016) CO₂ hydrogenation in a dielectric barrier discharge plasma revealed. *J Phys Chem C* 120:25210–25224. <https://doi.org/10.1021/acs.jpcc.6b07639>
44. Mei DH, Ashford B, He YL, Tu X (2017) Plasma-catalytic reforming of biogas over supported Ni catalysts in a dielectric barrier discharge reactor: Effect of catalyst supports. *Plasma Process Polym*. <https://doi.org/10.1002/ppap.201600076>
45. Duan XF, Hu ZY, Li YP, Wang BW (2015) Effect of Dielectric Packing Materials on the Decomposition of Carbon Dioxide Using DBD Microplasma Reactor. *AIChE J* 61:898–903. <https://doi.org/10.1002/aic.14682>
46. Zhu S, Zhou A, Yu F, Dai B, Ma C (2019) Enhanced CO₂ decomposition via metallic foamed electrode packed in self-cooling DBD plasma device. *Plasma Sci Technol* 21:085504. <https://doi.org/10.1088/2058-6272/ab15e5>
47. Jiang N, Lu N, Shang K, Li J, Wu Y (2013) Effects of electrode geometry on the performance of dielectric barrier/packed-bed discharge plasmas in benzene degradation. *J Hazard Mater* 262:387–393. <https://doi.org/10.1016/j.jhazmat.2013.08.072>
48. Ray D, Saha R, Subrahmanyam C (2017) DBD plasma assisted CO₂ decomposition: influence of diluent gases. *Catalysts* 7:244. <https://doi.org/10.3390/catal7090244>
49. Belov I, Paulussen S, Bogaerts A (2016) Appearance of a conductive carbonaceous coating in a CO₂ dielectric barrier discharge and its influence on the electrical properties and the conversion efficiency. *Plasma Sour Sci Technol*. <https://doi.org/10.1088/0963-0252/25/1/015023>
50. Mora EY, Sarmiento A, Vera E (2016) Vera, Alumina and quartz as dielectrics in a dielectric barrier discharges DBD system for CO₂ hydrogenation. *J Phys Conf Ser*. <https://doi.org/10.1088/1742-6596/687/1/012020>
51. Michielsen I, Uytendhouwen Y, Pype J, Michielsen B, Mertens J, Reniers F, Meynen V, Bogaerts A (2017) CO₂ dissociation in a packed bed DBD reactor: First steps towards a better understanding of plasma catalysis. *Chem Eng J* 326:477–488. <https://doi.org/10.1016/j.cej.2017.05.177>
52. Zhou A, Chen D, Ma C, Yu F, Dai B (2018) DBD plasma-ZrO₂ catalytic decomposition of CO₂ at low temperatures. *Catalysts* 8:256. <https://doi.org/10.3390/catal8070256>
53. Zeng Y, Tu X (2016) Plasma-catalytic CO₂ hydrogenation at low temperatures. *IEEE Trans Plasma Sci* 44:405–411. <https://doi.org/10.1109/TPS.2015.2504549>
54. Gallon HJ, Tu X, Whitehead JC (2012) Effects of reactor packing materials on H₂ production by CO₂ reforming of CH₄ in a dielectric barrier discharge. *Plasma Process Polym* 9:90–97. <https://doi.org/10.1002/ppap.201100130>
55. Chiper AS, Chen W, Mejlholm O, Dalgaard P, Stamate E (2011) Atmospheric pressure plasma produced inside a closed package by a dielectric barrier discharge in Ar/CO₂ for bacterial inactivation of biological samples. *Plasma Sour Sci Technol* 20:025008. <https://doi.org/10.1088/0963-0252/20/2/025008>
56. Xu Y, Jin H, Hirano T, Matsushita Y, Zhang J (2019) Characterization of Ni₃Sn intermetallic nanoparticles fabricated by thermal plasma process and catalytic properties for methanol decomposition. *Sci Technol Adv Mater* 20:622–631. <https://doi.org/10.1080/14686996.2019.1622447>
57. Lu N, Sun DF, Zhang CK, Jiang N, Shang KF, Bao XD, Li J, Wu Y (2018) CO₂ conversion in non-thermal plasma and plasma/g-C₃N₄ catalyst hybrid processes. *J Phys D Appl Phys* 51(9):094001. <https://doi.org/10.1088/1361-6463/aaa919>
58. Mei DH, Tu X (2017) Conversion of CO₂ in a cylindrical dielectric barrier discharge reactor: Effects of plasma processing parameters and reactor design. *J CO₂ Util* 19:68–78. <https://doi.org/10.1016/j.jcou.2017.02.015>
59. Mei D, He Y-L, Liu S, Yan J, Tu X (2016) Optimization of CO₂ conversion in a cylindrical dielectric barrier discharge reactor using design of experiments. *Plasma Process Polym* 13:544–556. <https://doi.org/10.1002/ppap.201500159>
60. Ozkan A, Dufour T, Silva T, Britun N, Snyders R, Bogaerts A, Reniers F (2016) The influence of power and frequency on the filamentary behavior of a flowing DBD—application to the splitting of CO₂. *Plasma Sour Sci Technol* 25(2):025013. <https://doi.org/10.1088/0963-0252/25/2/025013>
61. Ozkan A, Dufour T, Silva T, Britun N, Snyders R, Bogaerts A, Reniers F (2016) The influence of power and frequency on the filamentary behavior of a flowing DBD-application to the splitting of CO₂. *Plasma Sour. Sci. Technol* 25(2):025013. <https://doi.org/10.1088/0963-0252/25/2/025013>
62. Chaudhary R, van Rooij G, Li S, Wang Q, Hensen E, Hessel V (2020) Low-temperature, atmospheric pressure reverse water-gas shift reaction in dielectric barrier plasma discharge, with outlook to use in relevant industrial processes. *Chem Eng Sci* 225:115803. <https://doi.org/10.1016/j.ces.2020.115803>
63. Mei D, Zhu X, Wu C, Ashford B, Williams PT, Tu X (2016) Plasma-photocatalytic conversion of CO₂ at low temperatures: Understanding the synergistic effect of plasma-catalysis. *Appl Catal B* 182:525–532. <https://doi.org/10.1016/j.apcatb.2015.09.052>
64. Bogaerts A, Neyts E, Gijbets R, van der Mullen J (2002) Gas discharge plasmas and their applications. *Spectrochim Acta Part B* 57:609–658. [https://doi.org/10.1016/S0584-8547\(01\)00406-2](https://doi.org/10.1016/S0584-8547(01)00406-2)
65. Taghvaei H, Kheirollahivash M, Ghasemi M, Rostami P, Rahimpour MR (2014) Noncatalytic upgrading of anisole in an atmospheric DBD plasma reactor: effect of carrier gas type, voltage, and frequency. *Energy Fuels* 28:2535–2543. <https://doi.org/10.1021/ef402571j>
66. Zeng YX, Tu X (2017) Plasma-catalytic hydrogenation of CO₂ for the cogeneration of CO and CH₄ in a dielectric barrier discharge reactor: effect of argon addition. *J Phys D Appl Phys*. <https://doi.org/10.1088/1361-6463/aa64bb>
67. Liu L, Zhang Z, Das S, Xi S, Kawi S (2020) LaNiO₃ as a precursor of Ni/La₂O₃ for reverse water-gas shift in DBD plasma: Effect of calcination temperature. *Energy Convers Manage* 206:112475. <https://doi.org/10.1016/j.enconman.2020.112475>
68. Nakayama T, Ichikuni N, Sato S, Nozaki F (1997) Ni/MgO catalyst prepared using citric acid for hydrogenation of carbon dioxide. *Appl Catal A* 25:185–199. [https://doi.org/10.1016/S0926-860X\(96\)00399-7](https://doi.org/10.1016/S0926-860X(96)00399-7)
69. Xu S, Chansai S, Shao Y, Xu S, Wang YC, Haigh S, Mu Y, Jiao Y, Stere CE, Chen H, Fan X, Hardacre C (2020) Mechanistic study of non-thermal plasma assisted CO₂ hydrogenation over Ru supported on MgAl layered double hydroxide. *Appl Catal B* 268:118752. <https://doi.org/10.1016/j.apcatb.2020.118752>
70. Nizio M, Albarazi A, Cavadias S, Amouroux J, Galvez ME, Da Costa P (2016) Hybrid plasma-catalytic methanation of CO₂ at low temperature over ceria zirconia supported Ni catalysts. *Int J Hydrogen Energy* 41:11584–11592. <https://doi.org/10.1016/j.ijhydene.2016.02.020>
71. Nizio M, Benrabbah R, Krzak M, Debek R, Motak M, Cavadias S, Galvez ME, Da Costa P (2016) Low temperature hybrid plasma-catalytic methanation over Ni-Ce-Zr hydrotalcite-derived catalysts. *Catal Commun* 83:14–17. <https://doi.org/10.1016/j.catalcom.2016.04.023>
72. Zhou R, Rui N, Fan Z, Liu C-J (2016) Effect of the structure of Ni/TiO₂ catalyst on CO₂ methanation. *Int J Hydrogen Energy* 41:22017–22025. <https://doi.org/10.1016/j.ijhydene.2016.08.093>
73. Chen H, Mu Y, Shao Y, Chansai S, Xu S, Stere CE, Xiang H, Zhang R, Jiao Y, Hardacre C, Fan X (2019) Coupling non-thermal plasma with Ni catalysts supported on BETA zeolite for catalytic CO₂ methanation. *Catal. Sci Technol* 9:4135–4145. <https://doi.org/10.1039/C9CY00590K>

74. Lan L, Wang A, Wang Y (2019) CO₂ hydrogenation to lower hydrocarbons over ZSM-5-supported catalysts in a dielectric-barrier discharge plasma reactor. *Catal Commun* 130:105761. <https://doi.org/10.1016/j.catcom.2019.105761>
75. Xu W, Zhang X, Dong M, Zhao J, Di L (2019) Plasma-assisted Ru/Zr-MOF catalyst for hydrogenation of CO₂ to methane. *Plasma Sci Technol* 21:044004. <https://doi.org/10.1088/2058-6272/aaf9d2>
76. Xu W, Dong M, Di L, Zhang X (2019) A facile method for preparing UiO-66 encapsulated Ru catalyst and its application in plasma-assisted CO₂ methanation. *Nanomater*. <https://doi.org/10.3390/nano9101432>
77. Sivachandiran L, Costa PD, Khacef A (2020) CO₂ reforming in CH₄ over Ni/γ-Al₂O₃ nano catalyst: effect of cold plasma surface discharge. *Appl Sur Sci* 501:144175. <https://doi.org/10.1016/j.apsusc.2019.144175>
78. Aziz MAA, Jalil AA, Triwahyono S, Ahmad A (2015) CO₂ methanation over heterogeneous catalysts: recent progress and future prospects. *Green Chem* 17:2647–2663. <https://doi.org/10.1039/C5GC00119F>
79. Li W, Wang H, Jiang X, Zhu J, Liu Z, Guo X, Song C (2018) A short review of recent advances in CO₂ hydrogenation to hydrocarbons over heterogeneous catalysts. *Rsc Adv* 8:7651–7669. <https://doi.org/10.1039/C7RA13546G>
80. Liu HZ, Zou XJ, Wang XG, Lu XG, Ding WZ (2012) Effect of CeO₂ addition on Ni/Al₂O₃ catalysts for methanation of carbon dioxide with hydrogen. *J Nat Gas Chem* 21:703–707. [https://doi.org/10.1016/S1003-9953\(11\)60422-2](https://doi.org/10.1016/S1003-9953(11)60422-2)
81. Jin LJ, Li Y, Lin P, Hu HQ (2014) CO₂ reforming of methane on Ni/γ-Al₂O₃ catalyst prepared by dielectric barrier discharge hydrogen plasma. *Int J Hydrogen Energy* 39:5756–5763. <https://doi.org/10.1016/j.ijhydene.2014.01.171>
82. Jia X, Zhang X, Rui N, Hu X, Liu CJ (2019) Structural effect of Ni/ZrO₂ catalyst on CO₂ methanation with enhanced activity. *Appl Catal B* 244:159–169. <https://doi.org/10.1016/j.apcatb.2018.11.024>
83. Younas M, Loong Kong L, Bashir MJK, Nadeem H, Shehzad A, Sethupathi S (2016) Recent advancements, fundamental challenges, and opportunities in catalytic methanation of CO₂. *Energy Fuels* 30:8815–8831. <https://doi.org/10.1021/acs.energyfuels.6b01723>
84. Li Z, Zhao T, Zhang L (2018) Promotion effect of additive Fe on Al₂O₃ supported Ni catalyst for CO₂ methanation. *Appl Organomet Chem* 32:e4328. <https://doi.org/10.1002/aoc.4328>
85. Wierzbicki D, Moreno MV, Ognier S, Motak M, Grzybek T, Da Costa P, Gálvez ME (2019) Ni-Fe layered double hydroxide derived catalysts for non-plasma and DBD plasma-assisted CO₂ methanation. *Inter J Hydrogen Energy*. <https://doi.org/10.1016/j.ijhydene.2019.06.095>
86. Zhang Z, Ding H, Pan W, Ma J, Zhang K, Zhao Y, Song J, Wei C, Lin F (2023) Research progress of Metal-organic frameworks (MOFs) for CO₂ conversion in CCUS. *J Energy Inst*. <https://doi.org/10.1016/j.joei.2023.101226>
87. Sperling D (2007) Beyond oil and gas: the methanol economy. *Energy J* 28:178–179. <https://doi.org/10.1002/anie.200462121>
88. Olah GA (2004) After oil and gas: methanol economy. *Catal Lett*. <https://doi.org/10.1023/B:CATL.0000017043.93210.9c>
89. Olah GA, Goepfert A, Prakash GK (2009) Chemical recycling of carbon dioxide to methanol and dimethyl ether: from greenhouse gas to renewable, environmentally carbon neutral fuels and synthetic hydrocarbons. *J Org Chem* 74:487–498. <https://doi.org/10.1021/jo801260f>
90. Xu J, Su X, Liu X, Pan X, Pei G, Huang Y, Wang X, Zhang T, Geng H (2016) Methanol synthesis from CO₂ and H₂ over Pd/ZnO/Al₂O₃: catalyst structure dependence of methanol selectivity. *Appl Catal A* 514:51–59. <https://doi.org/10.1016/j.apcata.2016.01.006>
91. Chen WH, Lin BJ, Lee HM, Huang MH (2012) One-step synthesis of dimethyl ether from the gas mixture containing CO₂ with high space velocity. *Appl Energy* 98:92–101. <https://doi.org/10.1016/j.apenergy.2012.02.082>
92. Dubois JL, Sayama K, Arakawa H (1992) Conversion of CO₂ to dimethylether and methanol over hybrid catalysts. *Chem Lett* 21:1115–1118. <https://doi.org/10.1246/cl.1992.1115>
93. Alvarez A, Bansode A, Urakawa A, Bavykina AV, Wezendonk TA, Makkee M, Gascon J, Kapteijn F (2017) Challenges in the greener production of formates/formic acid, methanol, and DME by heterogeneously catalyzed CO₂ hydrogenation processes. *Chem Rev* 117:9804–9838. <https://doi.org/10.1021/acs.chemrev.6b00816>
94. Zhao J, Li YX, Zhu YQ, Wang Y, Wang CY (2016) Enhanced CO₂ photoreduction activity of black TiO₂-coated Cu nanoparticles under visible light irradiation: Role of metallic Cu. *Appl Catal A* 510:34–41. <https://doi.org/10.1016/j.apcata.2015.11.001>
95. Liao F, Huang Y, Ge J, Zheng W, Tedsree K, Collier P, Hong X, Tsang SC (2011) Morphology-dependent interactions of ZnO with Cu nanoparticles at the materials' interface in selective hydrogenation of CO₂ to CH₃OH. *Angew Chem* 50:2162–2165. <https://doi.org/10.1002/ange.201007108>
96. Deng K, Hu B, Lu Q, Hong X (2017) Cu/g-C₃N₄ modified ZnO/Al₂O₃ catalyst: methanol yield improvement of CO₂ hydrogenation. *Catal Commun* 100:81–84. <https://doi.org/10.1016/j.catcom.2017.06.041>
97. Li MMJ, Zeng ZY, Liao FL, Hong XL, Tsang SCE (2016) Enhanced CO₂ hydrogenation to methanol over CuZn nanoalloy in Ga modified Cu/ZnO catalysts. *J Catal* 343:157–167. <https://doi.org/10.1016/j.jcat.2016.03.020>
98. Wang ZJ, Song H, Pang H, Ning YX, Dao TD, Wang Z, Chen HL, Weng YX, Fu Q, Nagao T, Fang YM, Ye JH (2019) Photo-assisted methanol synthesis via CO₂ reduction under ambient pressure over plasmonic Cu/ZnO catalysts. *Appl Catal B* 250:10–16. <https://doi.org/10.1016/j.apcatb.2019.03.003>
99. Zhu S, Jiang B, Cai WB, Shao M (2017) Direct Observation on reaction intermediates and the role of bicarbonate anions in CO₂ electrochemical reduction reaction on Cu surfaces. *J Am Chem Soc* 139:15664–15667. <https://doi.org/10.1021/jacs.7b10462>
100. Luo W, Nie X, Janik MJ, Asthagiri A (2015) facet dependence of CO₂ reduction paths on Cu electrodes. *acs catal* 6:219–229. <https://doi.org/10.1021/acscatal.5b01967>
101. Perez-Gallent E, Figueiredo MC, Calle-Vallejo F, Koper MT (2017) Spectroscopic observation of a hydrogenated CO dimer intermediate during CO reduction on Cu(100) electrodes. *Angew Chem* 56:3621–3624. <https://doi.org/10.1002/anie.201700580>
102. Jiao Y, Zheng Y, Chen P, Jaroniec M, Qiao SZ (2017) Molecular scaffolding strategy with synergistic active centers to facilitate electrocatalytic CO₂ reduction to hydrocarbon/alcohol. *J Am Chem Soc* 139:18093–18100. <https://doi.org/10.1021/jacs.7b10817>
103. Ma S, Sadakiyo M, Heima M, Luo R, Haasch RT, Gold JL, Yamauchi M, Kenis PJ (2017) Electroreduction of carbon dioxide to hydrocarbons using bimetallic Cu-Pd catalysts with different mixing patterns. *J Am Chem Soc* 139:47–50. <https://doi.org/10.1021/jacs.6b10740>
104. Kattel S, Yan B, Yang Y, Chen JG, Liu P (2016) Optimizing binding energies of key intermediates for CO₂ hydrogenation to methanol over oxide-supported copper. *J Am Chem Soc* 138:12440–12450. <https://doi.org/10.1021/jacs.6b05791>

105. Luo Z, Tian SS, Wang Z (2020) Enhanced activity of Cu/ZnO/C catalysts prepared by cold plasma for CO_2 hydrogenation to methanol. *Ind Eng Chem Res* 59:5657–5663. <https://doi.org/10.1021/acs.iecr.9b06996>

Publisher's Note Springer Nature remains neutral with regard to jurisdictional claims in published maps and institutional affiliations.

Springer Nature or its licensor (e.g. a society or other partner) holds exclusive rights to this article under a publishing agreement with the author(s) or other rightsholder(s); author self-archiving of the accepted manuscript version of this article is solely governed by the terms of such publishing agreement and applicable law.